Asociación Argentina
de Mecánica Computacional

Mecánica Computacional Vol XXXIV, págs. 2889-2901 (artículo completo)
Sebastián Giusti, Martín Pucheta y Mario Storti (Eds.)
Córdoba, 8-11 Noviembre 2016

IDENTIFICATION OF THE TENSILE FORCE IN A CABLE WITH INSULATORS USING A BAYESIAN APPROACH

Bruno J. Rango[a,b], **Fernando J. Serralunga**[a], **Marta B. Rosales**[a,b] **and Marcelo T. Piován**[b,c]

[a]*Departamento de Ingeniería, Universidad Nacional del Sur, Av. Alem 1253, 8000 Bahía Blanca, Argentina, brunorango@gmail.com, fjserralunga@uns.edu.ar, mrosales@criba.edu.ar*

[b]*CONICET, Argentina*

[c] *Grupo Análisis de Sistemas Mecánicos, Universidad Tencológica Nacional - Facultad Regional Bahía Blanca, Argenina, mpiovan@frbb.utn.edu.ar*

Keywords: Cable, insulators, Bayesian statistics, tension inference

Abstract. Guyed towers are common structural types of extended use in the communication industry. In some cases, due to technical requirements, insulators are necessary. One of the techniques to estimate the pretension force in a cable is through the measurement of its natural frequencies and the related code standards include specific formulae. However, the presence of the insulators leads to a different situation which is not considered in the codes. In this paper, a Bayesian approach is applied to the identification of the tensile force in a prestressed cable with insulators. Firstly, a physical model of the cable is constructed in the laboratory. A high speed camera is used to register the displacements of the structure undergoing free vibrations. The videos are analysed using a specific software and the time series response is obtained. With this information, the natural frequencies of the cable with insulators are evaluated. Additionally, a Finite Element model of the cable is built. Then, the Bayes rule is implemented through Markov-Chain Monte-Carlo (MCMC) simulations and, as a result, the probability distribution of the cable tension is obtained. The estimates are compared with the true value of the tensile force acting on the physical configuration of the cable. Finally, the uncertainties in the inferred values are propagated through the computational model and the frequency response is evaluated.

1 INTRODUCTION

Cable supported structures are extensively used in the Civil Engineering. Their applications go from urban power transmission lines and advertising banners to more complex configurations such as guyed towers, high power transmission lines and bridges. The tensile force of the cables is determined at the design stage and the stability of the structure is highly influenced by this value. For this reason, it is essential to accurately measure this force at the moment of assemblage of the structure as well as during its service lifespan. Several techniques based on structural dynamics for monitoring the cable tension have been developed and applied. In this sense, some authors (Fu et al., 2004; Ren et al., 2005) have addressed the study of the dynamical behaviour of bridge cables. In particular, the second paper deals with the development of an empirical formula relating natural frequencies with the tensile force. In the same way, (Kim and Park, 2007) present a comparative study of the application of six different methods for the estimation of the force in cables of suspension bridges. However, these techniques are conditioned by the uncertainty in the resulting values and by the impossibility of application in a variety of civil structures. In particular, some configurations of guyed towers which present insulators attached along the cables, lie out of the scope of application of the existing techniques.

In this context, Bayesian statistics constitutes an interesting approach to certain kind of inverse problems. The approach consists on using observed data to update the available previous knowledge with respect to one or various parameters of the system. These kind of methods are widely used in the context of structural mechanics. Some authors (Beck and Yuen, 2004; Mthembu et al., 2011) make use of the Bayesian approach for model selection. However, the most usual application of the Baysian methods in the fields of structural mechanics is related to damage detection. Glaser et al. (2007), for instance, implement the Bayes rule based on static data, to detect representative changes in the parameters of a cantilever beam which are indicative of the flaw. On the other hand, Moore et al. (2011, 2012) report the Bayesian identification of the crack parameters in a plate using time series data of the structure undergoing free vibrations. In particular, in the second paper, the results are compared with the response of an experimental model. In the same way, Lam et al. (2007) use transient vibration data for detecting the location and depth of multiple cracks in a cantilever beam. Ritto et al. (2016) study the decreasing stiffness of the clamped side of a cantilever beam by means of a Markov-Chain Monte Carlo approach, based on frequency measurements obtained from a physical model. Apart from damage detection, model based Bayesian methods prove to be useful in the identification of parameters which are difficult to measure in the practice. In this sense, Ritto (2014) reports the inference of the parameters that govern the dynamics of the bit-rock interaction of a drill string used in oil and gas industries.

In the present paper, the inference of the tensile force in a cable with insulators is addressed. For this purpose, a Bayesian approach based on natural frequencies data is adopted. The procedure is repeated using the first one, two and three natural frequencies in turn. A forward model based in the Finite Element Method (FEM) is constructed using a commercial software. The posterior probability distribution of the tensile force, given the experimental data, is computed through a Markov-Chain Monte Carlo implementation of the Bayes rule. The 90% confidence interval of the results is reported. Additionally, the uncertainties in the tensile force are propagated through the FEM model and the distribution of the frequencies is computed. These distributions are then compared to the experimentally measured frequencies. The method proves to perform adequately and it is shown that, as expected, the more experimental information supplied, the better the inference.

2 COMPUTATIONAL MODEL

The Bayesian procedure adopted for the inference problem in this paper, requires the repeated execution of the computational model of the mechanical system. The model is constructed in COMSOL Multiphysics® (2015), a FEM based software adequate for physics and engineering applications. The simulations are performed using the *LiveLink*^{TM} *for Matlab*®, an extension of COMSOL which allows to integrate both programs. Thus, the results can be easily post-processed in Matlab.

2.1 Description of the model

A scheme of the mechanical system is depicted in Fig. 1. It consists of a stranded steel cable pinned at both ends. The tilt angle relative to the horizontal is $\theta = 60°$. Two insulators are placed at the thirds of the total length $L = 2$ m. The cable tensile force T constitutes the unknown model parameter to be inferred.

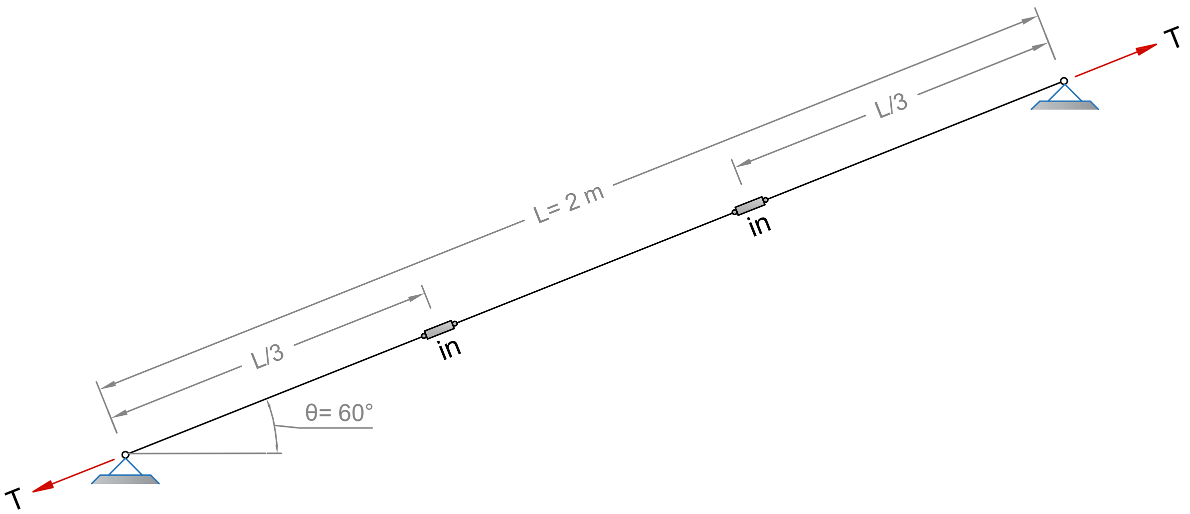

Figure 1: Taut cable with two insulators.

In the context of COMSOL, the study *Prestressed Analysis, Eigenfrequency* available for the *truss* and *beam* interfaces using the *Structural Mechanics* module, is performed. Such study consists of two stages: first, the static load is applied (*i.e.*, the self-weight of the cable and the insulators and the axial tensile force); in the second stage, the eigenfrequencies of the structure prestressed according to the load state from step one, are computed.

Truss elements with initial stress are adopted for the cable. The insulators, on the other hand, are modelled using beam elements. Additionally, a point mass is placed at each end node of the insulator, to simulate the usual fixing clamps. The corresponding material properties for each element are defined under the *Linear Elastic Material* node. The *Initial stress and strain* node is enabled, and the initial stress σ_0 is settled as a function of the tensile force parameter: $\sigma_0 = T/A$. Then, the geometrical properties of the elements are established under the *Cross section data* node. Self-weight is modelled as a distributed force per unit length both for the cable and the insulators. Finally, the essential boundary conditions are applied by setting the pinned condition to the nodes at both ends of the cable. The mesh size is selected automatically, resulting in 20 truss elements of four degrees of freedom (two in-plane displacements at each node) for the cable and a single beam element of six degrees freedom (two in-plane displacements and a rotation at each node) for each insulator. Before running the program, the *Include geometric Nonlinearities* option under the *Study* node must be checked in order to account for large deformations.

3 EXPERIMENTAL PROCEDURE

A series of dynamic experiments was performed to measure the first three natural frequencies on a physical model of the cable with insulators. In Fig. 2, the experimental setup is shown. It consists of an inclined stranded (19 wires) stainless steel cable of diameter $d = 15$ mm with two insulators placed at the thirds of the total length $L = 2$ m. The lower end was attached to a tensioning screw placed on a rigid frame, whereas the upper end was fixed to a S-type load cell which registered the applied tensile force. Regarding the insulators, they were constructed using rectangular Polymethyl Methacrylate (PMMA) parallelepipeds. Their shape and connection to the cable were conceived to simulate the ceramic egg-shaped insulators used in the guy wires of some particular configurations of guyed masts. Small steel clamps were used to fix the insulators.

Figure 2: Experimental model of the cable with two insulators.

First, the desired tensile force was applied operating the tensioning screw. Then, the static configuration of equilibrium was disturbed by a manual perturbation. A Casio Exilim EX-FS10 high speed camera was used to record the displacements of a point of the cable undergoing free vibrations. The records were taken during 4 seconds at 420 frames per second. Then, using the free video analysis software Tracker 4.94 (2016), the dynamics of the experiment were reconstructed and the time series displacements response was obtained. The *autotracker* functionality of the software allows to automatically track a video feature of interest (see Fig. 3). For this purpose, a red circular marker of negligible weight had previously been attached to the cable at the point of interest. In this way, a time series of the in-plane transverse displacements of the cable was registered. The obtained data was exported and processed in Matlab where the time domain representation of the signal was deconstructed into the frequency domain using the Fast Fourier Transform (FFT). In Fig. 4, the time domain response of a particular test is shown. Furthermore, in Fig. 5 the frequency domain representation of the signal is depicted. The natural frequencies of the cable were determined by identifying the highest peaks from the FFT graph. With the aim of performing a better estimation and considering the measurement uncertainties inherent to any physical experiment, the test was repeated 5 times and the results were averaged. The mean values $\bar{f}_1 = 9.43$ Hz, $\bar{f}_2 = 17.72$ Hz and $\bar{f}_3 = 56.72$ Hz were adopted as the experimental frequencies to be used in the Bayesian framework.

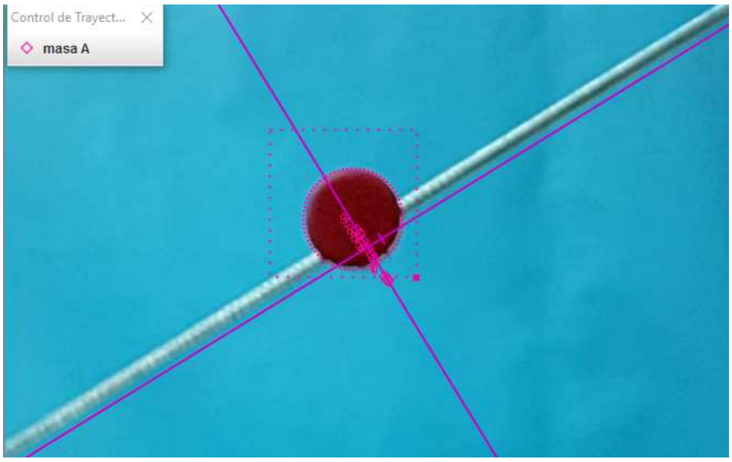

Figure 3: Autotracking of the marker attached to the cable using Tracker.

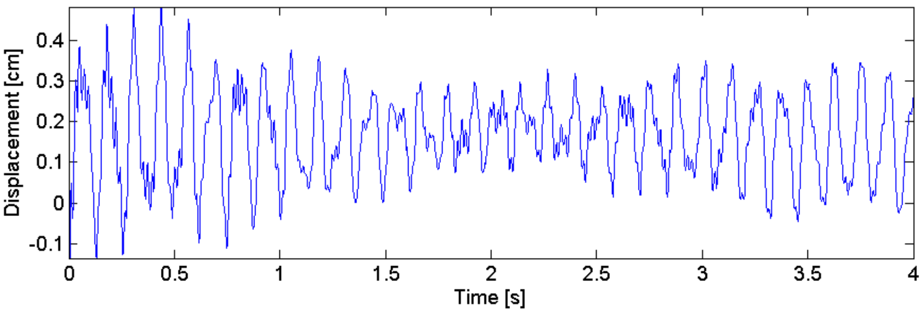

Figure 4: Measured response in the time domain.

4 BAYESIAN INFERENCE

In this section, the Bayesian inverse approach is described (see for example Kaipio and Somersalo (2006) and Gelman et al. (2013)). Based on the data observed experimentally, we want to infer which is the tensile force that caused those frequencies. For this purpose, a forward model $f_{num}(T)$ to simulate the observed frequencies is available (see Section 2). However, the computational and experimental models differ by some amount. To account for this discrepancy, an error is modelled as additive and mutually independent of the parameter of interest T. In particular, a Gaussian white noise $\mathcal{N}(0, \sigma^2)$ is assumed. Thus, for a given value of the tensile force, the observed frequencies f_{exp} can be expressed according to Eq. 1 where $f(T)$ is a vector containing the corresponding frequencies calculated with the FEM based model and n is

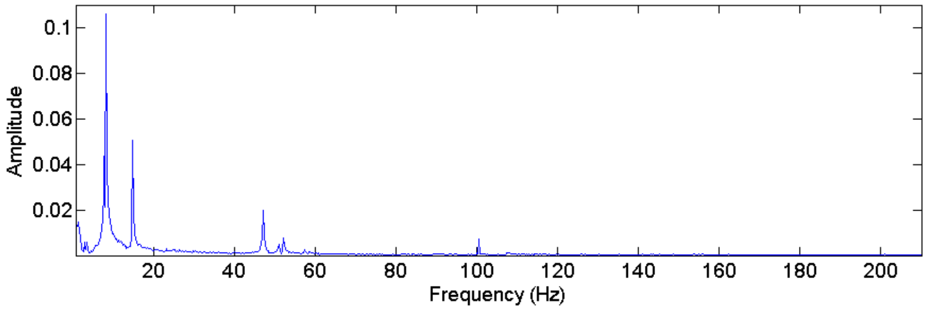

Figure 5: Measured response in the frequency domain (FFT).

a realization of the noise model.

$$f_{exp} = f_{num}(T) + n \tag{1}$$

The function through which the prior knowledge is updated based on the data is called the *likelihood*. It expresses the conditional probability of having observed the experimental data. Because there is no analytic expression for this function, we can evaluate it by means of the numeric model. On the basis of Eq. 1, the probability that the measured frequencies were simulated by the numerical model with tensile force T is distributed like the noise $\mathcal{N}$. Therefore, the likelihood distribution is expressed according to:

$$p_L(f_{exp}|T) = \frac{1}{\sqrt{2\pi\sigma^2}} \exp\left(-\frac{(f_{exp} - f_{num}(T))^2}{2\sigma^2}\right). \tag{2}$$

On the other hand, every previous knowledge about the parameter to be inferred is expressed as the prior probability distribution $p_{prior}(T)$. In this study, the only thing we know about the tensile force is that it can not be negative nor higher than the ultimate tensile strength of the cable $T_s = 2560$ N. Therefore, this lack of knowledge is expressed by assigning the same probability to every possible value, which results in a Uniform prior distribution in the interval [0,T_s].

Once the prior and the likelihood distributions are defined, we can infer the posterior probability distribution of the tensile force $p_{posterior}(T|f)$ by means of the Bayes rule:

$$p_{posterior}(T|f) = \frac{p_L(f_{exp}|T)\, p_{prior}(T)}{p(f)} \tag{3}$$

where the term $p(f)$ is a normalizing constant. It ensures that the area under the posterior probability distribution equals one. As will be discussed later, there is no need for evaluating its expression.

4.1 Evaluation of the posterior distribution

The next step is to sample from the posterior distribution. For this purpose, the Markov Chain Monte Carlo (MCMC) methods arise as particularly suitable. MCMC simulation is based on sampling sequentially, in order to construct a Markov Chain where each sample depends only on the value of the previous. As the number of iterations increases, the Markov Chain converges to a stationary distribution which is the posterior $p_{posterior}(T|y)$ (Gelman et al., 2013). For the present problem, the implementation of the Bayes rule is performed by means of the MCMC - Metropolis Hastings (MH) algorithm (Metropolis et al., 1953; Hastings, 1970). One of the main strengths of the method lies in the lax requirements on the distribution to sample from: it has to be known up to a constant. Therefore, for the case of Bayesian inference there is no need to compute the normalizing constant $p(f)$ in Eq. 3. Consequently, the Bayes rule can now be expressed as

$$p_{posterior}(T|f) \propto p_L(f|T)\, p_{prior}(T). \tag{4}$$

The MCMC-MH algorithm proceeds as follows:

1. Initialize the chain by selecting the starting point T^0 and set $i = 1$;
2. Generate a sample T^* form the user-defined proposal distribution $q(T|T^{i-1})$;
3. Compute the probabilities ratio $r = \frac{p_{posterior}(T^*|f)}{p_{posterior}(T^{i-1}|f)} \frac{q(T^{i-1}|T^*)}{q(T^*|T^{i-1})}$;
4. Generate a random value u from the uniform distribution $\mathcal{U}(0, 1)$
5. If $r > u$ set $T^i = T^*$; otherwise keep $T^i = T^{i-1}$;
6. Go back to step 2 and repeat the sequence for $i = 2, ..., N_S$, where N_S is the number of samples in the chain.

5 RESULTS

The results herein reported correspond to three separate implementations of the Bayesian framework, using different amount of experimental data in each case. This scheme is adopted considering the fact that in the field it would be straightforward to measure only the first natural frequency, for technical and operational reasons. However, in order to evaluate the potential of the method in terms of estimation accuracy, more experimental information is desired. Therefore, the amount of data supplied is decreased from three frequencies to one. The different cases are were identified according to Table 1.

Case	**Experimental data** $[Hz]$
A	$\bar{f}_1 = 9.43$, $\bar{f}_2 = 17.72$, $\bar{f}_3 = 56.72$
B	$\bar{f}_1 = 9.43$, $\bar{f}_2 = 17.72$
C	$\bar{f}_1 = 9.43$

Table 1: Identification of the data in the different cases considered.

In all the cases, the MCMC-MH algorithm was implemented through the Matlab function *mhsample( )*. A Normal distribution centred at the previous accepted sample and truncated into $T \in [0, T_s]$ is used as *proposal* $q()$. Its variance σ_q^2 is chosen so that the acceptance rate be close to the optimal value of 0.44 (Gelman et al., 2013). The starting point of the chain T^0 is randomly selected by the user and is the same in all the cases. To prevent the chain from being influenced by this initial value, the early iterations are discarded. This phase is called the burn-in. The evolution of the sampler during this period is shown in Fig. 6 for all the cases. The dashed red line corresponds to the true tensile force acting on the experimental configuration of the cable. In cases A and B, the convergence of the MCMC chain towards the stationary state during the burn-in phase is made explicit by the approach of the samples towards the true value during the first 100 simulations. However, in case C, the samples fluctuate with considerable amplitude around the red line. For this reason, a conservative solution is adopted and the length of the burn-in period is increased to 1000 samples. This behaviour will be further discussed later.

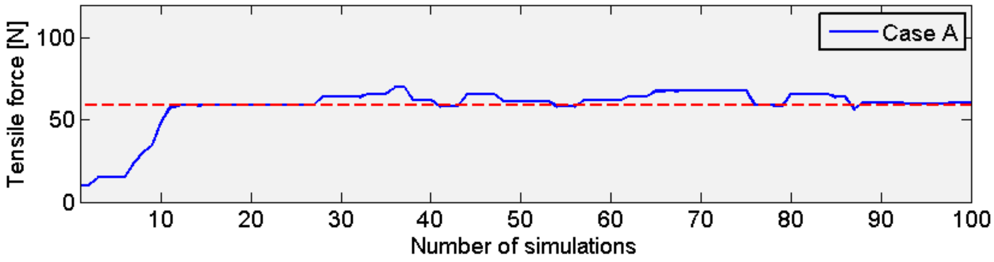

(a) Case A

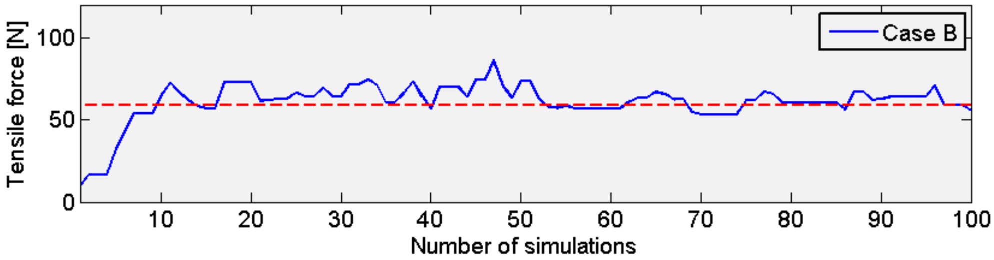

(b) Case B

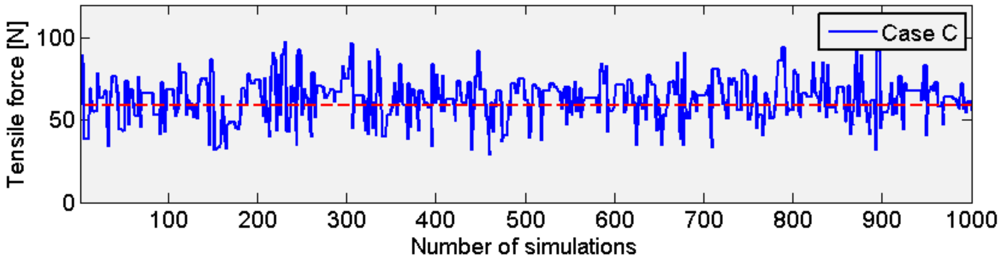

(c) Case C

Figure 6: Evolution of the sampler during the burn-in period.

Once the burn-in period is completed, the iterative MCMC process is continued for 5000 additional simulations and the new samples are assumed to belong to the stationary MCMC chain. Therefore, the *ksdensity()* Matlab function is used to approximate the PDF of the inferred parameter. The posterior PDF for all the cases is plotted in Fig. 7 and identified by colors. The vertical dashed red line corresponds to the actual tensile force applied to the cable in the laboratory. The PDF of case A is remarkably narrower than those of case B and C, which implies higher confidence in the results when the whole set of experimental data is used. As expected, the curves become wider as the size of the observed data is reduced, due to higher dispersion in the value of the samples. It is worth noting that, independently of the size of the data, the curves are shifted to the right of the red line.

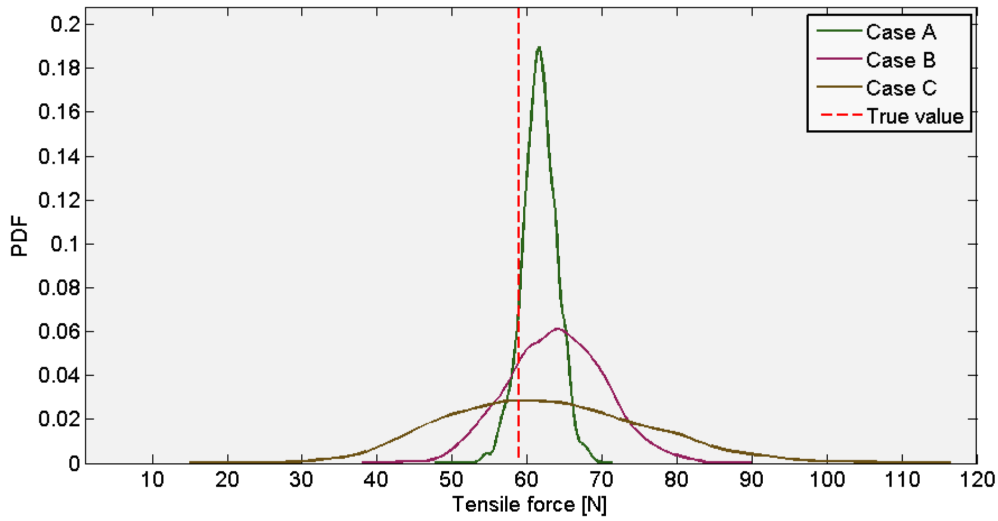

Figure 7: Posterior probability distribution of the tensile force for cases A, B, and C.

In order to evaluate quantitatively the observations discussed in the previous paragraph, the following point and interval estimates are introduced (Kaipio and Somersalo, 2006). The Maximum a posteriori (MAP) is a point estimate of the mode of the posterior distribution, defined by Eq. 5. Given that the three posterior distributions are unimodal, the MAP constitutes an appropriate estimate for this problem. Likewise, a usual point estimate is constituted by the Conditioned Mean (CM) of the inferred parameter conditioned on the data (Eq. 6). Regarding the posterior uncertainty, a common interval measure is the Central Posterior Probability (CPP). In this study, the 90% CPP interval is reported. It is defined by the range of values inside which the 90% of the posterior probability lies. This interval is obtained from the Cumulative Density Function (CDF) of the posterior distribution corresponding to each case. The three cumulative distributions are depicted in Fig. 8.

$$MAP = arg\ max\ (p_{posterior}(T|f)) \tag{5}$$

$$CM = E\{T|f\} = \int T \cdot p_{posterior}(T|f)dT \tag{6}$$

The MAP, the CM, the 90% CPP interval and the standard deviation (SD) corresponding to the three posterior distributions are summarized in Table 2. Additionally, the error relative to the true value (TV) of the tensile force is computed for the MAP and CM point estimates as

$$\begin{aligned} e_{r1} &= \frac{MAP - TV}{TV}; \\ e_{r2} &= \frac{CM - TV}{TV}. \end{aligned} \tag{7}$$

The estimates of the tensile force are good for the three cases. As expected, the highest level of confidence in the estimates is achieved when the whole set of experimental data is used (case A). Moreover, in case A, the MAP and CM estimates are equally good, and the 90% CPP interval is appropriately narrow.

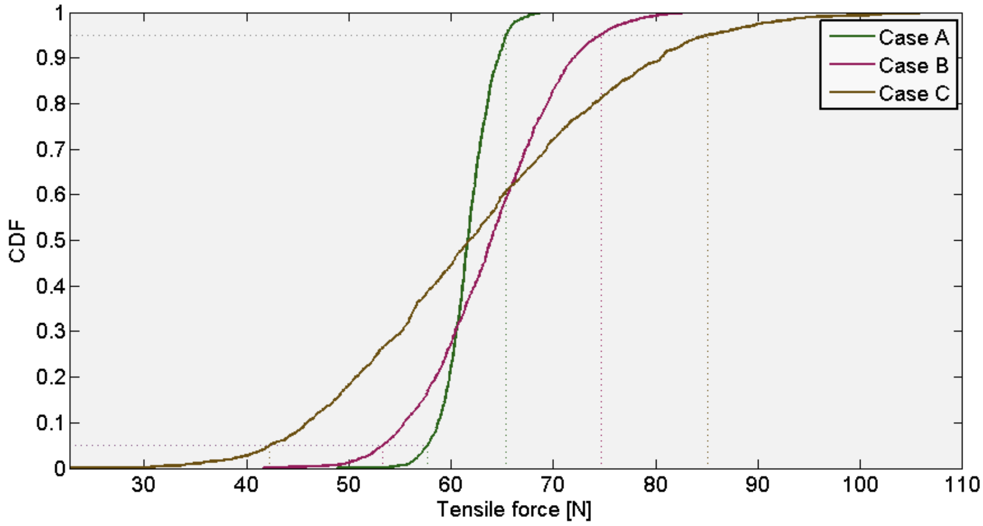

Figure 8: Cumulative density function (CDF) of the posterior distribution for cases A, B and C. Determination of the 90% CPP intervals.

Case	**MAP** [N]	$e_{r1}(\%)$	**CM** [N]	$e_{r2}(\%)$	**90% CPP** [N]	**SD** [N]
A	61.6	*4.4*	61.6	*4.4*	57.7 < T < 65.4	2.3
B	64.1	*8.6*	63.9	*8.3*	53.3 < T < 74.6	6.4
C	59.0	*0.0*	62.5	*5.9*	42.2 < T < 85.1	13.3

Table 2: Point and interval estimates of the posterior distribution: Maximum a Posteriori (MAP), Conditioned Mean (CM), 90% Central interval of Posterior Probability (CPP), and Standard Deviation (SD). The relative errors are computed with respect to the true value $TV =$ 59 N.

An interesting result is obtained in case C: the MAP estimate exhibits the lowest relative error (in fact, a zero value is obtained). However, due to the the variability of the values sampled, the CM estimate does not sustain that result but exhibits the third highest relative error. The discrepancy between both point estimates is explained by the wide range of 90% CPP interval and the high value of the standard deviation. An unexpected result is that case B leads to the least accurate MAP and CM estimates. Anyway, the magnitude of the relative error obtained in this case is acceptable for practical applications. On the other side, according to the 90% credible interval reported for case B, using two frequencies instead of one leads to a higher degree of confidence in the results.

Regarding the high uncertainty in the estimates when only the first natural frequency is taken into account (case C), the possibility of reducing the dispersion at the expense of a higher computational cost has been considered. However, when the convergence of the MCMC sampler is analysed (Fig. 9), it results evident that the convergence has already been achieved. The reason for the variability in the samples can be explained if the behaviour of the FEM model is studied. This is: if a variation of the tensile force is applied to the model, the corresponding variation of the first natural frequency computed is very small. For example, if the tensile force is increased from 55 to 65 N, the first natural frequency varies 0.76 Hz whereas the third varies 4.65 Hz.

Therefore, when only the first natural frequency is used for the implementation MCMC algorithm, regions of high probability are explored for a wide range of values of the tensile force. For this same reason, the information provided by the third natural frequency is relevant and leads to a significant reduction of the dispersion.

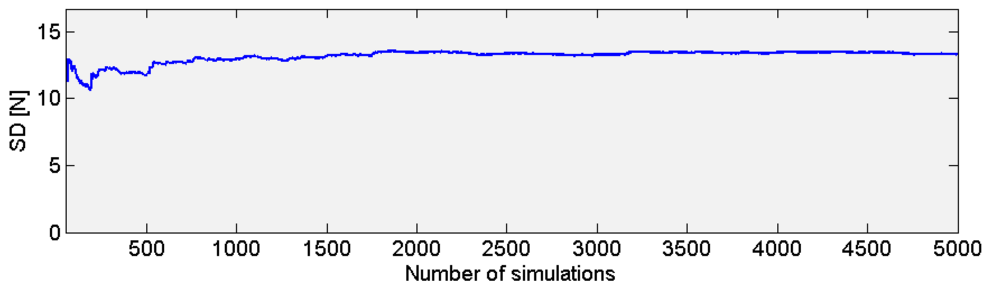

Figure 9: Convergence of the MCMC-MH sampler evaluated in terms of the Standard Deviation (Case C).

5.1 Uncertainty Quantification (UQ)

Finally, the uncertainties in the inferred values are propagated through the FEM model in order to study the frequency response in the three cases. First, a number of the generated samples are selected according to the shape of the posterior distribution. Then, each one of these samples are input into the numerical model and the corresponding natural frequencies of the prestressed cable are computed. The resulting probability distributions are shown in Fig. 10 (a)-(c), for cases A, B and C respectively. The dashed vertical line indicates the value of the frequencies measured experimentally as described in Section 3. The experimental frequency, as well as the mean and the SD of each distribution are reported at the top of the figures.

It is worth noting that the mean is uniformly close to the experimental frequency in the three cases and for all the frequencies. On the other hand, the SD is less uniform along the different cases. For instance, the SD of the distribution of the first natural frequency in case A is significantly lower than in cases B and C. This is an expected result, because the posterior distribution of tensile force of case A also exhibits the lowest dispersion.

6 CONCLUSION

The existing methods for estimating the tensile force in cables are not applicable to cable with insulators, which are frequent configurations in guyed towers. For this reason, the inference of the tensile force in a cable with two insulators is addressed in the present paper.

A Bayesian framework is adopted for the problem. The method is based on updating the prior knowledge regarding the parameter of interest using observed data. In particular, the first three natural frequencies of a physical model are measured experimentally. This data is used in conjunction with a forward FEM based model to perform an MCMC implementation of the Bayes rule. The procedure is repeated three times using different amounts of experimental data.

The posterior distributions of the unknown parameter is constructed and compared to the true value of tensile force applied to the cable. Point and interval estimates are reported. The results are more credible as the size of the experimental data is reduced. However, the estimates obtained in the three cases are admissible for practical applications. In summary, the performance of the method is promising for the solution of this problem on the real scale.

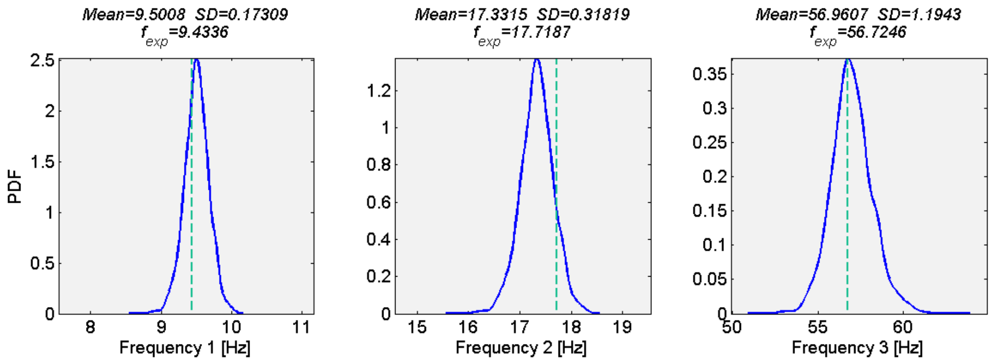

(a) Case A

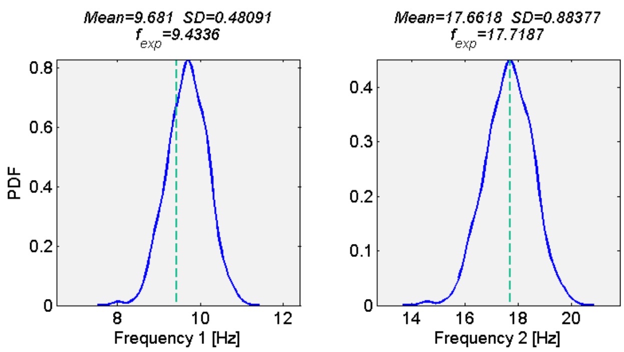

(b) Case B

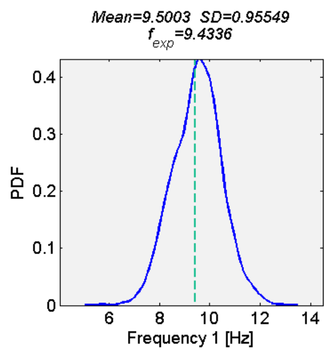

(c) Case C

Figure 10: Probability distributions of the natural frequencies obtained from the UQ study. The Mean and the Standard Deviation (SD) of the distributions, together with the frequencies measured experimentally (f_{exp}) are reported at the top of the figures (expressed in Hz).

REFERENCES

Beck J.L. and Yuen K.V. Model selection using response measurements: Bayesian probabilistic approach. *Journal of Engineering Mechanics*, 130(2):192–203, 2004.

COMSOL Multiphysics®. http://www.comsol.com/, 2015.

Fu Q., Deng Y., and Mao L. Wireless measurement system of cable tension force based on labview. *SICE Anual Conference in Sapporo, Japan*, 2004.

Gelman A., Carlin J., Stern H., Dunson D., Vehtari A., and Rubin D. *Bayesian Data Analysis, Third Edition*. Chapman & Hall/CRC Texts in Statistical Science. Taylor & Francis, 2013. ISBN 9781439840955.

Glaser R.E., Lee C.L., Nitao J.J., Hickling T.L., and Hanley W.G. Markov chain monte carlo-based method for flaw detection in beams. *Journal of Engineering Mechanics*, 133(12):1258–1267, 2007.

Hastings W.K. Monte carlo sampling methods using markov chains and their applications. *Biometrika*, 57(1):97–109, 1970.

Kaipio J. and Somersalo E. *Statistical and Computational Inverse Problems*. Applied Mathematical Sciences. Springer New York, 2006. ISBN 9780387271323.

Kim B. and Park T. Estimation of cable tension force using the frequency-based system identification method. *Journal of Sound and Vibration*, 304:660–676, 2007.

Lam H., Ng C., and Veidt M. Experimental characterization of multiple cracks in a cantilever beam utilizing transient vibration data following a probabilistic approach. *Journal of Sound* *and Vibration*, 305(1-2):34–49, 2007.

Metropolis N., Rosenbluth A.W., Rosenbluth M.N., Teller A.H., and Teller E. Equation of state calculations by fast computing machines. *The Journal of Chemical Physics*, 21(6):1087, 1953.

Moore E.Z., Murphy K.D., and Nichols J.M. Crack identification in a freely vibrating plate using bayesian parameter estimation. *Mechanical Systems and Signal Processing*, 25(6):2125–2134, 2011.

Moore E.Z., Nichols J.M., and Murphy K.D. Model-based SHM: Demonstration of identification of a crack in a thin plate using free vibration data. *Mechanical Systems and Signal Processing*, 29:284–295, 2012.

Mthembu L., Marwala T., Friswell M.I., and Adhikari S. Model selection in finite element model updating using the bayesian evidence statistic. *Mechanical Systems and Signal Processing*, 25(7):2399–2412, 2011.

Ren W., Chen G., and Hu W. Empirical formulas to estimate cable tension by cable fundamental frequency. *Structural Engineering and Mechanics*, 20:363–80, 2005.

Ritto T., Sampaio R., and Aguiar R. Uncertain boundary condition bayesian identification from experimental data: A case study on a cantilever beam. *Mechanical Systems and Signal Processing*, 68-69:176–188, 2016.

Ritto T.G. Bayesian approach to identify the bit–rock interaction parameters of a drill-string dynamical model. *Journal of the Brazilian Society of Mechanical Sciences and Engineering*, 37(4):1173–1182, 2014.

Tracker 4.94. Video analysis and modeling tool by douglas brown. http://www.cabrillo.edu/~dbrown/tracker, 2016.